

NATO ASI Series

Advanced Science Institutes Series

A series presenting the results of activities sponsored by the NATO Science Committee, which aims at the dissemination of advanced scientific and technological knowledge, with a view to strengthening links between scientific communities.

The series is published by an international board of publishers in conjunction with the NATO Scientific Affairs Division

A	Life Sciences	Plenum Publishing Corporation New York and London
B	Physics	
C	Mathematical and Physical Sciences	Kluwer Academic Publishers Dordrecht, Boston, and London
D	Behavioral and Social Sciences	
E	Applied Sciences	
F	Computer and Systems Sciences	Springer-Verlag Berlin, Heidelberg, New York, London, Paris, and Tokyo
G	Ecological Sciences	
H	Cell Biology	

Recent Volumes in this Series

Volume 181—Fundamental Processes of Atomic Dynamics

edited by J. S. Briggs, H. Kleinpoppen, and H. O. Lutz

Volume 182—Physics, Fabrication, and Applications of Multilayered Structures

edited by P. Dhez and C. Weisbuch

Volume 183—Properties of Impurity States in Superlattice Semiconductors

edited by C. Y. Fong, Inder P. Batra, and S. Ciraci

Volume 184—Narrow-Band Phenomena—Influence of Electrons with Both Band and Localized Character

edited by J. C. Fuggle, G. A. Sawatzky, and J. W. Allen

Volume 185—Nonperturbative Quantum Field Theory

edited by G. 't Hooft, A. Jaffe, G. Mack,
P. K. Mitter, and R. Stora

Volume 186—Simple Molecular Systems at Very High Density

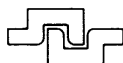
edited by A. Polian, P. Loubeyre, and N. Boccara

Volume 187—X-Ray Spectroscopy in Atomic and Solid State Physics

edited by J. Gomes Ferreira and M. Teresa Ramos

Volume 188—Reflection High-Energy Electron Diffraction and Reflection Electron Imaging of Surfaces

edited by P. K. Larsen and P. J. Dobson



Series B: Physics

Bayerische
Staatsbibliothek
München

Reflection High-Energy Electron Diffraction and Reflection Electron Imaging of Surfaces

Edited by

P. K. Larsen

Philips Research Laboratories
Eindhoven, The Netherlands

and

P. J. Dobson

Philips Research Laboratories
Redhill, United Kingdom

Plenum Press

New York and London

Published in cooperation with NATO Scientific Affairs Division

Proceedings of a NATO Advanced Research Workshop
on Reflection High-Energy Electron Diffraction
and Reflection Electron Imaging of Surfaces,
held June 15-19, 1987,
in Veldhoven, The Netherlands

Library of Congress Cataloging in Publication Data

NATO Advanced Research Workshop on Reflection High-Energy Electron Diffraction
and Reflection Electron Imaging of Surfaces (1987: Veldhoven, Netherlands)

Reflection high-energy electron diffraction and reflection electron imaging of
surfaces / edited by P. K. Larsen and P. J. Dobson.

p. cm.—(NATO ASI series. Series B, Physics; v. 188)

“Proceedings of a NATO Advanced Reserach Workshop on Reflection High-
Energy Electron Diffraction and Reflection Electron Imaging of Surfaces, held
June 15-19, 1987, in Veldhoven, The Netherlands”—T.p. verso.

“Published in cooperation with NATO Scientific Affairs Division.”

Includes bibliographical references and index.

ISBN 0-306-43035-5

1. Surfaces (Physics)—Technique—Congresses. 2. Reflection high energy
electron diffraction—Congresses. 3. Reflection electron microscopy—Con-
gresses. I. Larsen, P. K. II. Dobson, P. J. III. North Atlantic Treaty Organization.
Scientific Affairs Division. IV. Title. V. Series.

QC173.4.S94N37 1987

88-28843

530.4'1—dc19

CIP

© 1988 Plenum Press, New York
A Division of Plenum Publishing Corporation
233 Spring Street, New York, N.Y. 10013

All rights reserved

No part of this book may be reproduced, stored in a retrieval system, or transmitted
in any form or by any means, electronic, mechanical, photocopying, microfilming,
recording, or otherwise, without written permission from the Publisher

Printed in the United States of America

SPECIAL PROGRAM ON CONDENSED SYSTEMS OF LOW DIMENSIONALITY

This book contains the proceedings of a NATO Advanced Research Workshop held within the program of activities of the NATO Special Program on Condensed Systems of Low Dimensionality, running from 1983 to 1988 as part of the activities of the NATO Science Committee.

Other books previously published as a result of the activities of the Special Program are:

- Volume 148 **INTERCALATION IN LAYERED MATERIALS**
edited by M. S. Dresselhaus

- Volume 152 **OPTICAL PROPERTIES OF NARROW-GAP LOW-DIMENSIONAL STRUCTURES**
edited by C. M. Sotomayor Torres, J. C. Portal, J. C. Maan, and R. A. Stradling

- Volume 163 **THIN FILM GROWTH TECHNIQUES FOR LOW-DIMENSIONAL STRUCTURES**
edited by R. F. C. Farrow, S. S. P. Parkin, P. J. Dobson, J. H. Neave, and A. S. Arrott

- Volume 168 **ORGANIC AND INORGANIC LOW-DIMENSIONAL CRYSTALLINE MATERIALS**
edited by Pierre Delhaes and Marc Drillon

- Volume 172 **CHEMICAL PHYSICS OF INTERCALATION**
edited by A. P. Legrand and S. Flandrois

- Volume 182 **PHYSICS, FABRICATION, AND APPLICATIONS OF MULTILAYERED STRUCTURES**
edited by P. Dhez and C. Weisbuch

- Volume 183 **PROPERTIES OF IMPURITY STATES IN SUPERLATTICE SEMICONDUCTORS**
edited by C. Y. Fong, Inder P. Batra, and S. Ciraci

CONTENTS

SURFACE STRUCTURAL DETERMINATION

EXPERIMENTAL

- Experimental Overview of Surface Structure Determination
by RHEED
S. Ino 3

THEORY

- Surface Structural Determination Using RHEED
J.L. Beeby 29
- Theory of RHEED by Reconstructed Surfaces
M.G. Knibb and P.A. Maksym 43
- Accurate Dynamical Theory for RHEED Rocking-curve Intensity
Spectra
S.Y. Tong, T.C. Zhao and H.C. Poon 63

INELASTIC EFFECTS

- Inelastic Scattering Effects in RHEED and Reflection Imaging
A.L. Bleloch, A. Howie, R.H. Milne and M.G. Walls 77
- Excitation of Dielectric Spheres by Electron Beams
P.M. Echenique 91

RESONANCE AND CHANNELING EFFECTS

- Resonance Effects in RHEED
G. Meyer-Ehmsen 99
- Inelastic Scattering and Secondary Electron Emission Under
Resonance Conditions in RHEED from Pt(111)
H. Marten 109
- Adatom Site Determination Using Channeling Effects in RHEED
on X-ray and Auger Electron Production
J.C.H. Spence and Y. Kim 117

A Note on the Bloch Wave and Integral Formulations of RHEED Theory Jon Gjønnes	131
---	-----

DISORDERS AND STEPS IN ELECTRON DIFFRACTION

Diffraction from Disordered Surfaces: An Overview M.G. Lagally, D.E. Savage and M.C. Tringides	139
Theory of Electron Scattering from Defect: Steps on Surfaces with Non-equivalent Terraces W. Moritz	175
Diffraction from Stepped Surfaces M. Henzler	193
RHEED and Disordered Surfaces B. Bölger, P.K. Larsen and G. Meyer Ehmsen	201
Temperature Diffuse Scattering in RHEED M. Albrecht and G. Meyer-Ehmsen	211
Temperature Dependence of the Surface Disorder on Ge(001) Due to Ar ⁺ Ion Bombardment A.J. Hoeven, J.S.C. Kools, J. Aarts and P.C. Zalm	217
Two-dimensional First-order Phase Separation in an Epitaxial Layer T.-M. Lu and S.-N. Yang	225

CONVERGENT BEAM DIFFRACTION

Surface Convergent-Beam Diffraction for Characterization and Symmetry Determination J.A. Eades and M.D. Shannon	237
Convergent Beam RHEED Calculations Using the Surface Parallel Multislice Approach A.E. Smith	251

REFLECTION ELECTRON MICROSCOPY

USING CONVENTIONAL INSTRUMENTS

Reflection Electron Microscopy in TEM and STEM Instruments J.M. Cowley	261
Reflection Electron Microscopy with Use of CTEM: Studies of Au Growth on Pt(111) K. Yagi, S. Ogawa and Y. Tanishiro	285
Application of Reflection Electron Microscopy for Surface Science (observation of cleaned crystal surfaces of Si, Pt, Au and Ag) Y. Uchida	303
Reflection Microscopy in a Scanning Transmission Electron Microscope R.H. Milne	317

Contrast of Surface Steps and Dislocations Under Resonance, Non-resonance, Bragg, and Non-Bragg Conditions Tung Hsu and L.-M. Peng	329
MICROPROBE RHEED	
Microprobe Reflection High-energy Electron Diffraction M. Ichikawa and T. Doi	343
Scanning RHEED Studies of Silicide Formation in a UHV-SEM P.A. Bennett and A.P. Johnson	371
LOW ENERGY INSTRUMENTS	
Low Energy Electron Reflection Microscopy (LEEM) and Its Application to the Study of Si Surfaces E. Bauer and W. Telieps	381
Low Energy Scanning Electron Microscope T. Ichinokawa	385
ELECTRON DIFFRACTION STUDIES OF GROWTH	
SEMICONDUCTORS	
RHEED Intensity Oscillations During MBE Growth of III-V Compounds - An Overview B.A. Joyce, J.H. Neave, J. Zhang and P.J. Dobson	397
RHEED Oscillations Control of GaAs and AlAs MBE Growth Using Phase-lock Modulated Beams F. Briones, L. Gonzalez and J.A. Vela	419
The Contribution of Atomic Steps to Reflection High energy Electron Diffraction from Semiconductor Surfaces P.R. Pukite, P.I. Cohen and S. Batra	427
RHEED Studies of Growing Ge and Si Surfaces J. Aarts and P.K. Larsen	449
LEED Investigations of Si MBE onto Si(100) M. Horn, U. Gotter and M. Henzler	463
METALS	
Quantitative Studies of the Growth of Metals on GaAs(110) Using RHEED D.E. Savage and M.G. Lagally	475
RHEED Intensity Oscillations in Metal Epitaxy G. Lilienkamp, C. Koziol and E. Bauer	489
THEORY	
Calculation of RHEED Intensity from Growing Surfaces T. Kawamura	501
Studies of Growth Kinetics on Surfaces with Diffraction M.C. Tringides and M.G. Lagally	523
Index	539

THEORY OF ELECTRON SCATTERING FROM DEFECT: STEPS
ON SURFACES WITH NON-EQUIVALENT TERRACES

W. Moritz

Institut f. Kristallographie und
Mineralogie Universitaet Muenchen
Theresienstr. 41, 8000 Muenchen 2, FRG

INTRODUCTION

One important parameter for the characterization of surfaces is the surface roughness. The density and distribution of steps influences most of the physical and chemical properties of surfaces. It is found, for example, that a number of catalytic reactions at surfaces actually take place at edge or kink sites. In the production of semiconductor devices the flatness of surfaces or interfaces plays an essential role. Therefore a number of techniques have been developed to investigate the topography of surfaces either by direct imaging or by diffraction using both, X-rays and electrons. The diffraction method is the most convenient method to obtain information about the surface roughness on an atomic scale.

The quantities which are easily obtained from a diffraction experiment are average quantities like terrace widths, island size distribution functions, mean roughness depths etc., because usually a large area of the surface is probed. The determination of the details of the atomic geometry at and around a defect or a step usually requires a large experimental and theoretical effort because of lack of sensitivity to such details, and in the case of electron diffraction, because multiple scattering effects become important.

Surface roughness, domain or island distributions cause broadening of the diffracted beams, in general depending on the diffraction conditions and the beam indices. In many cases only the width of the beam (full width at half maximum) is measured as an estimate of the average island or terrace size. However, from an analysis of the angular beam profiles the size distribution can be obtained. This is usually done in the kinematic approximation (single scattering) where the calculation of beam profiles becomes especially easy. The kinematical theory is used for low energy electron diffraction (LEED) as well as for reflection high energy electron diffraction (RHEED). Although multiple scattering effects are in general strong for electron diffraction, for the calculation of angular beam profiles the kinematical theory is in many cases sufficient. The question arises whether multiple scattering can always be neglected in evaluating beam profiles and what effects occur. In the case of LEED with its back scattering geometry, multiple scattering effects are short ranged and the kinematic evaluation of angular beam profiles is usually based on that argument. For RHEED with its high electron energies and the occurrence of

forward scattering this argument should be less applicable. On the other hand, large terrace sizes can be measured with a RHEED instrument using the low index beams where the resolution is high. In such cases multiple scattering effects should again be negligible. In general, for RHEED multiple scattering effects are more disturbing in the beam profile analysis than for LEED and in addition, shadowing effects occur.

Multiple scattering effects can be divided into two parts, one where the multiple scattering path crosses a domain boundary or a step and another part where this is not the case and multiple scattering occurs only within one domain and within the bulk. The latter effect is in general strong and cannot be neglected, neither for LEED nor for RHEED, but is not relevant for the angular beam profiles if only antiphase domains exist at the surface. Therefore it is usually not considered in the analysis of beam profiles from stepped surfaces where all terraces are equivalent. At surfaces with non-equivalent terraces it can be treated in a simple quasi-kinematical approximation as will be discussed below. The other contribution to the multiple scattering effect, where subsequent scattering in different terraces is involved, is certainly important for RHEED but requires a more sophisticated treatment than that given here and is not considered in this article.

Diffraction from stepped surfaces has been described in a number of studies dealing with one dimensional distributions [1-8]. The reference list is not intended to be complete, an extensive list of references can be found in the review article by Lagally et al. [9]. It is usually assumed that the surface consist of terraces of identical scattering properties but separated by a shift vector with vertical and lateral components. This is in general the case for all unreconstructed surfaces of the monoatomic lattices including the fcc and bcc metals. The (111) surface of the diamond lattice also exhibits only one type of terrace, whereas the (100) surface similar to the basal plane of the hcp lattice, consists of two different terminations. Non-equivalent terraces may be the inherent property of the lattice or the result of reconstruction. The Si(100) surface, for example, has two rotational domains due to the four-fold screw axis of the bulk lattice which reduces to a two-fold axis at the surface. These two different domains exist even without a reconstruction. Another example is the W(100) surface where the reduction of the symmetry in a single domain is due to the reconstruction. The four-fold symmetry of the unreconstructed surface is destroyed by atomic displacements and two rotational domains occur in addition to the antiphase domains. It is in such cases that the effect of multiple scattering within one terrace cannot be neglected for the calculation of beam profiles even for the specular beam. In a kinematic calculation, where only single scattering is considered, the structure factor of the specular beam would be the same for all domains. Therefore a distribution of rotational domains would not cause a broadening of the specular beam. This is not so in case of multiple scattering. Here the structure factors for rotational domains can be very different. Neglecting different structure factors at the domain boundaries (and shadowing effects etc.) the surface can be approximately described by domains with different structure factors. That means the surface consists of domains, or in the case of Si(100) of terraces, which for electrons differ in the effective scattering properties. These terraces are therefore denoted in the following as non-equivalent terraces, though the actual structures may be symmetrically equivalent. That the diffraction from rotational domains or terraces has to be described by different structure factors is clearly a multiple scattering effect and would not occur, for example, in the specular beam with X-ray diffraction. This effect is large and depends strongly on the diffraction conditions as can be easily seen from the experimental rotational diagrams where large intensity variations occur.

In the case of LEED, rotational diagrams could even be used for structure analysis. Azimuthal dependencies of intensities and beam profiles have also been reported in RHEED studies [10-13].

The diffraction from stepped surfaces with non-equivalent terraces can be easily described by a quasi-kinematic approximation by assuming different structure factors for each kind of terrace and using the kinematic formalism otherwise. Multiple scattering effects arising from scattering paths within one terrace and within the bulk are included in this way. Those multiple scattering paths crossing a step are neglected here. This is of course an approximation but it is well applicable for LEED at surface with large terraces and elucidates also some of the effects observed with RHEED.

In the next chapter the diffraction from stepped surfaces will be discussed from the very general consideration that the diffracted intensity can be divided into two parts, one arising from long range order and the other from short range order. The influence of the existence of two different terraces on the intensity oscillations during layer by layer growth is discussed briefly and a detailed calculation of beam profiles which would be expected from a Si(100) surface with single and double steps and a geometric distribution of terrace widths is given.

GENERAL ASPECTS OF DIFFUSE SCATTERING

The intensity scattered from a disordered structure can be divided into two terms, a sharp reflection and a diffuse intensity. The sharp reflection is due to the ordered lattice and exists as long range order exists. The range is given by the resolution limit of the instrument. The diffuse intensity arises from the fluctuation of the scattering amplitudes along the surface,

$$\begin{aligned}
 I(\underline{k}, \underline{k}') = & \left| \sum_{n=1}^N \bar{F}(\underline{k}, \underline{k}') e^{i(\underline{k} - \underline{k}') \cdot \underline{R}_n} \right|^2 + \\
 & \sum_{n=1}^N \sum_{n'=1}^N [(F_n(\underline{k}, \underline{k}') - \bar{F}(\underline{k}, \underline{k}')) (F_n^*(\underline{k}, \underline{k}') - \bar{F}^*(\underline{k}, \underline{k}'))] \times \quad (1) \\
 & \times e^{i(\underline{k} - \underline{k}') \cdot (\underline{R}_n - \underline{R}_{n'})}
 \end{aligned}$$

where \underline{R}_n is a two dimensional lattice vector, N is the number of unit cells, \underline{k} and \underline{k}' are the wave vectors of the incoming and outgoing waves and $F_n(\underline{k}, \underline{k}')$ are structure amplitudes to unit cell column values. $\bar{F}(\underline{k}, \underline{k}')$ is the spatial average of structure amplitudes. To simplify the above expression we assume that the structure amplitudes are slowly varying functions of the diffraction angle. It may be further assumed that the density of defects or steps is low so that multiple scattering effects at the edges can be neglected. The diffracted intensity can then be approximately written in the convenient form

$$\begin{aligned}
 I(\underline{k}, \underline{k}') = & |\bar{F}|^2 G(h) G(k) + N(|\bar{F}|^2 - |\bar{F}|^2) P(\underline{k} - \underline{k}') \quad (2) \\
 G(x) = & \frac{\sin^2 N_1 \pi x}{\sin^2 \pi x}
 \end{aligned}$$

where $P(\underline{k} - \underline{k}')$ is the Fourier transform of the pair-correlation functions and describes the angular beam profile, h and k are the beam indices. N

is the total number of unit cells. Eqs. 1 or 2 describe that the intensity in the sharp reflections is due to the mean value of the scattering amplitudes and that the integrated diffuse intensity is proportional to the mean square deviation of scattering amplitudes.

A comment has to be made on multiple scattering effects. It should be noted that Eq. 1 is in general valid, also for the multiple scattering case, when for each unit cell at the lattice point \underline{R}_n an individual structure factor is taken according to the individual surroundings of the unit cell. Eq. 2 is in general not valid because it neglects all multiple scattering effects between different terraces or islands if $P(\underline{k} - \underline{k}')$ is the Fourier-transform of the pair-correlation functions. It corresponds to the column approximation used in high energy electron diffraction [14]. A general multiple scattering formulation has to include multi-site correlations. The applicability of Eq. 2 is justified by the fact that for an exponential decay of pair correlation functions, all multi-site correlation functions will also exhibit the same exponential decay. As long as no sharp interferences in the scattering factors occur, the beam profiles will therefore keep the Lorentzian form as in the kinematic case. This has also been shown analytically for one dimension [3,15]. It has to be kept in mind further that in the kinematic limit the total integrated intensity remains constant independent of the state of order while in the multiple scattering theory this is in general not the case. Interference in the multiple scattering paths can drastically enhance the intensity of a certain beam. The intensity, of course, is then missing in other beams. Conservation of the total diffracted intensity cannot be observed, however, because only the backscattering part can be measured. Furthermore, strong absorptive effects depending on the diffraction conditions destroy the conservation of the integrated intensity.

It is often convenient to start with Eq. 2 for a qualitative discussion of the characteristic features of the diffraction pattern. If uncorrelated defects exist at the surface the diffuse intensity will be uniformly distributed over the reciprocal unit cell, the angular distribution being determined only by the angular dependence of the atomic cross section. If the defect atoms form clusters or terraces, the diffuse intensity will be concentrated around certain points in the reciprocal unit cell. The intensity of the sharp reflection as well as the diffuse intensity may vanish at certain points, i.e., the mean value of the scattering amplitudes vanishes for a surface with an equal distribution of terraces at the "out of phase" condition. The mean square deviation may also vanish, e.g., at in phase scattering from two different terraces, and usually has its maximum when the mean value has its minimum. The qualitative features of the diffraction patterns for the two simple cases as shown in the Figures 1-4 follows directly from the interpretation of Eq. 2.

The intensity and angular profile of the specular beam for a two level system as a function of coverage and momentum transfer perpendicular to the surface is displayed in Figures 1 and 2. It is assumed here that the two terraces are equivalent. This case has been described in detail and has been frequently verified experimentally [4-9] but will be shortly repeated here for the sake of completeness. Thus the two levels have scattering factors $F_1(\underline{k}, \underline{k}')$ and $F_2(\underline{k}, \underline{k}')$ differing by a phase factor

$$F_2(\underline{k}, \underline{k}') = F_1(\underline{k}, \underline{k}') e^{i(\underline{k} - \underline{k}') \underline{d}} \quad (3)$$

$$|F_2(\underline{k}, \underline{k}')| = |F_1(\underline{k}, \underline{k}')|$$

where \underline{d} is the shift vector between terraces. The mean value of the scattering factor at coverage Θ is defined as

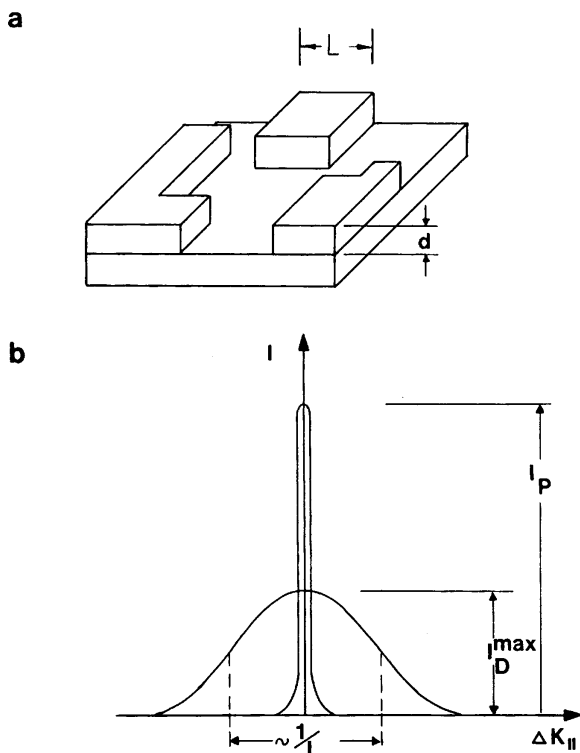


Fig. 1. Model of a surface with identical terraces in two levels and the corresponding angular profile of the specular beam. The beam profile consists in general of two components, a central peak and a diffuse part. The width of the diffuse intensity corresponds roughly to the mean terrace size.

$$\bar{F}(\underline{k}, \underline{k}') = (1 - \theta)F_1(\underline{k}, \underline{k}') + \theta F_2(\underline{k}, \underline{k}') \quad (4)$$

and the intensity of the central peak is

$$I_p = |F_1|^2 [1 - 2\theta(1 - \theta)(1 - \cos 2\pi s)] \quad (5)$$

where $s = (\underline{k} - \underline{k}')d/2\pi$ is the momentum transfer in reciprocal lattice units. The arguments \underline{k} and \underline{k}' have been dropped for convenience. The integral diffuse intensity is given by

$$I_D = 2\theta(1 - \theta) |F_1|^2 (1 - \cos 2\pi s). \quad (6)$$

The peak intensity becomes an oscillating function in reciprocal space as well as being a function of coverage as illustrated in Figure 2a-c. The minimum of the peak intensity of the specular beam corresponds to half coverage. Because at this point the diffraction from all layers should be out of phase, the intensity of the sharp reflection has to vanish. The remaining intensity at $s = 1/2$ is therefore entirely due to the maximum of the diffuse term and corresponds roughly to the square of the average island diameter. The width of the diffuse intensity in reciprocal units is approximately the inverse of the island diameter, the exact value depends on the island size distribution function. How the maximum of the diffuse intensity behaves as a function of coverage cannot be generally given in this qualitative discussion since this depends on the specific

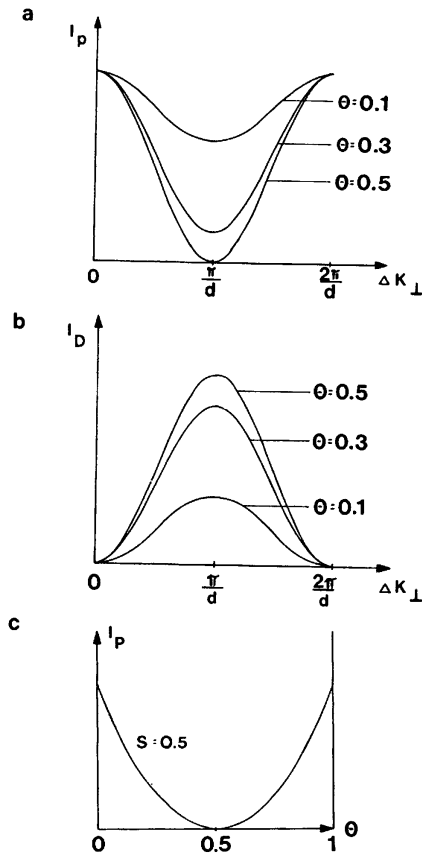


Fig. 2. Intensity oscillations as a function of coverage and momentum transfer. Intensity of the central peak (a) and diffuse part (b) at different coverages. c: Intensity of the central peak as a function of coverage at the "out of phase" condition, $s = 1/2$, where $(\underline{k} - \underline{k}')d = 2\pi s$.

growth model. At each maximum of the central peak one layer is completed. The layer growth mechanism is obviously best studied at the "out of phase" condition where the maximum effect on the peak intensity and diffuse intensity is observed. From the slope of the peak intensity at full coverage (Figure 2c) the number of layers involved in the growth process can be determined [16].

We consider next a surface with non-equivalent terraces and assume also layer by layer growth. We assume further that the surface with a complete layer consists of one terrace only, see Figure 3a. The structure amplitudes for both terraces differ now in modulus and phase in addition to the geometric phase

$$F_1 = |F_1| e^{i\phi_1(\underline{k}, \underline{k}')} , F_2 = |F_2| e^{i\phi_2(\underline{k}, \underline{k}')} \quad (7)$$

$$|F_1| \neq |F_2| .$$

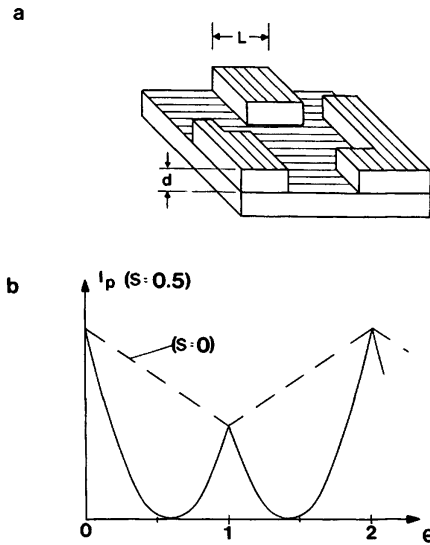


Fig. 3. a. Model of a surface with two non-equivalent terraces in two levels. b. Intensity oscillations of the central peak as a function of coverage. Solid line: "out of phase" condition, broken line: "in phase" condition. A relation of $|F_1|^2 = 0.5|F_2|^2$ has been assumed. A phase factor between the complex structure amplitudes F_1 and F_2 influences only the "in phase" and "out of phase" conditions but not the positions of maxima and minima on the coverage scale.

The mean value of scattering amplitudes does not vanish any more at the out of phase condition ($s = 1/2$) and at half coverage. Also the maxima and minima may be shifted due to the phase difference. The peak intensity is now given by

$$I_p = (1 - \theta)^2 |F_1|^2 + \theta^2 |F_2|^2 + 2\theta(1 - \theta) |F_1 F_2| \cos(2\pi s + \Delta\phi) \quad (8)$$

and shows now a double periodicity as a function of coverage, Figure 3b. The integral diffuse intensity is

$$I_D = \theta(1 - \theta) [|F_1|^2 + |F_2|^2 - 2|F_1 F_2| \cos(2\pi s + \Delta\phi)] \quad (9)$$

and cannot show a double periodicity as a function of coverage as it results from the mean square deviation in structure amplitudes. This case is illustrated in Figure 4a and b. The phase difference $\Delta\phi(\underline{k}, \underline{k}')$ between the structure factors shifts the maxima and minima of the intensity of the central peak away from the points $s = 0$ and $s = 1/2$. The same occurs for the maxima and minima of the diffuse intensity in reciprocal space according to Eqs. 8 and 9. It should be noted that a double periodicity in reciprocal space for the peak intensity or angular width, which has been observed for Si(100) at incidence in [011] direction [17], is due to the existence of four levels with two rotational domains and two antiphase domains. The simpler system which is illustrated in Figures 3 and 4 consists of only two levels.

The intensity oscillations as observed with RHEED or LEED during layer by layer growth (see Figure 3b) exhibit a double periodicity but still have a maximum and minimum at full coverage because the diffuse term

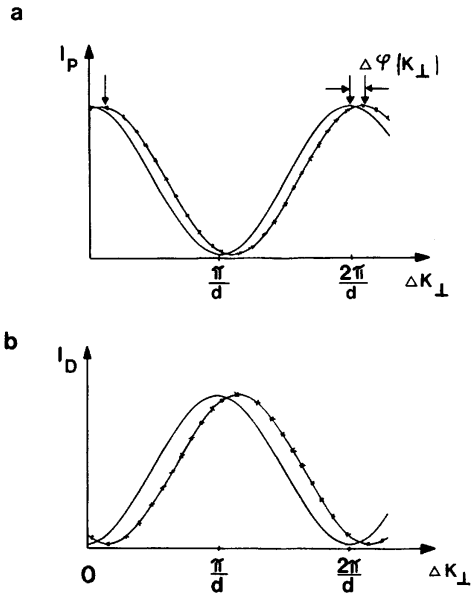


Fig. 4. Intensity oscillations of the peak intensity and the diffuse intensity for two different terraces and half coverage as a function of momentum transfer. $|F_1|^2 = 0.5|F_2|^2$. The phase difference $\Delta\phi(\underline{k}, \underline{k}')$ shifts the position of maxima and minima in reciprocal space.

always vanishes at full coverage. The intensity oscillations as a function of momentum transfer s and coverage θ are now different. It is interesting to note that double periodicities and azimuthal dependencies of intensity oscillations during MBE growth of Si(100) [11,12,18] and GaAs(100) [10,13] have been observed. From the above discussion follows that the shift of maxima and minima in the intensity oscillations as observed during MBE growth of Si(100) and GaAs(100) cannot be explained only with a sequence of two different layers. The occurrence of two maxima during the completion of only one layer has obviously to be explained by a strongly peaked diffuse scattering at half coverage [10]. On the other hand, the fact that at certain diffraction conditions, the intensity initially increases with increasing coverage, as has been observed for GaAs(100) [10], follows directly from the assumption of a phase difference between the two scattering factors. For the Si(100) surface the azimuthal dependence of the intensity oscillations has been explained by multiple scattering effects involving the form of the growing terraces [19].

At special diffraction conditions the structure factors of the two terraces can become equal, that is when the plane of incidence coincides with a symmetry plane transforming one terrace to the other. For the Si(100) surface this occurs for incidence in the [010] direction. The two terraces have then identical scattering factors for the specular beam. This is not so at incidence in the [011] direction, for which scattering factors are different. The dependence of the structure factor on the azimuthal angle is specific for multiple scattering. From the above discussion, it follows that the Si(100) surface looks like a two level

surface with equivalent terraces at observation in [010] and with non-equivalent terraces in the [011] direction. The double and single periodicities in reciprocal space at different azimuths have indeed been observed experimentally [17,20]. Double periodicity in the oscillation of beam widths has also been observed for Os(0001) [21] and has been interpreted by the existence of double steps.

It is highly unrealistic to assume that the area of the surface illuminated by the primary beam consists of only one or two terraces, unless the beam is very well focused. Usually a superposition of all possible domains corresponding to the point symmetry of the crystal is observed in the diffraction pattern. For GaAs(100) or Si(100), for example, the two orientations of the (4 x 2) and (2 x 1) structures respectively, are always observed unless one orientation is suppressed at vicinal faces. For the above mentioned case of a two layer sequence this means that the scattering amplitudes from two regions of the surface have to be summed up with alternate layer sequences. This superposition can be done coherently or incoherently. The latter implies that large areas exist where one layer is completed before the next begins to grow. The doubling of the period of the peak intensity with increasing coverage (Figure 3b) is then removed. If a double periodicity is observed, however, it can be concluded that only one domain is present within the area of the incident beam. Experimentally this has been observed for Si(100), see the article by Horn et al. in this volume, Figure 1.

The other case, coherent superposition, corresponds to the simultaneous growth of four layers which may not be realized at steady state conditions but may occur for the initial growth conditions. This will not be discussed here because it depends too much on the specific model for the initial terrace width distribution and the specific growth model that general conclusions can be drawn from the qualitative picture used above. The coherent superposition of the scattering amplitudes from four levels, however, and the consequences for the beam widths in reciprocal space will be discussed for the Si(100) surface in some detail in the next section.

It has been assumed up to now that the surface is flat and consists of only two levels at least within the coherence length of the electrons which may be as large as several μ . It has been shown experimentally that these assumptions are justified for many cases of molecular beam epitaxy including the case of Si(100) [18]. However, the situation where the surface is rough on an atomic scale, which means that many levels exist within the coherence length of the beam, is also quite frequently realized, and the consequences for the beam profiles can be shortly mentioned. For a two level system, see Figure 1, the beam profile consists of two components, a central peak and a diffuse part. The intensity of the central peak vanishes only at certain points in reciprocal space and at certain coverages. The width of the diffuse part remains independent of the diffraction conditions and depends only on the island distribution. As the number of different levels increases, the intensity of the central peak decreases rapidly as a function of momentum transfer and additional narrow diffuse features occur [4]. In the limiting case of an infinite number of levels, a surface which is rough on an atomic scale, the central peak vanishes at all diffraction conditions except at the Bragg-condition where all levels scatter "in phase". The width of the peak then broadens continuously. This has been shown previously in an analysis of the beam profiles of the disordered Au(110) surface [3]. The influence of the number of levels on the beam profiles has also been investigated in detail recently [6-8].

ONE DIMENSIONAL MODEL WITH SINGLE AND DOUBLE STEPS

The calculation of beam profiles from one-dimensional disordered surfaces with a geometric distribution of steps follows the methods developed for the analysis of stacking faults in crystals [22-24] and the application to steps on surfaces has been described in detail previously [3-8]. Therefore the formalism will be only shortly repeated here as far as it is necessary to include double steps. So far most calculations of beam profiles from stepped surfaces have assumed single steps occurring at the surface with a given probability α . That model includes the occurrence of double steps with the probability α^2 and assumes that there is no correlation between steps. A slightly modified model where the occurrence of a double step is given a different probability β and how this will become visible in the beam profiles will be investigated here. To assume a different probability for the occurrence of double steps within the formal frame of a geometric distribution of terrace sizes is possible because four different terraces, or four levels, are assumed.

The Si(100) surface has been found to show a preference for double steps. Vicinal surfaces form double steps as has been concluded from the fact that only one orientation of the reconstructed (2 x 1) unit cell occurs [25,26]. The existence of double steps has been observed recently in the direct image with Reflection Electron Microscopy (REM) [27] and Transmission Electron Microscopy (TEM) [28]. The formation of double steps has also been predicted theoretically [24]. It is therefore interesting to investigate how double steps can be observed in the beam profiles. The 1-D model with a geometric distribution of steps will be applied here because of its simplicity. The Lorentzian shape of the beam profile resulting from the exponential decay of correlations has been found often to fit the experimental profiles sufficiently well [4]. The exponential decay of correlations corresponds in 1-D to the geometric distribution of terrace widths. The 1-D model has the advantage that the beam profiles can be calculated analytically and the influence of different parameters can be easily seen. The 1-D model is also useful for the description of vicinal faces. It is not expected that the general features of the diffraction patterns and beam profiles differ substantially from the exact calculation for the 2-D model. For a quantitative evaluation of terrace size distributions, however, a two-dimensional calculation may be necessary.

Two limiting cases can be distinguished. First the case of a four level surface, corresponding to the four layer sequence in the bulk of Si(100) with two different probabilities for single and double steps. This is the limiting case of a flat surface showing all four types of domains. The other limiting case is a rough surface with an infinite number of layers (at a laterally infinite surface) and continuously broadened beams. At special diffraction conditions, that is at "in phase" and "out of phase" scattering from single step height terraces, both cases result in the same beam profiles. In the model discussed below a rough surface is assumed by allowing the occurrence of up and down steps in each level.

A model of the Si(100) surface with the four different terraces is shown in Figure 5. The direction of the edges is assumed to be along the densely packed atomic rows in [011]. There are two antiphase domains and two rotational domains in the four terraces having structure factors

$$\begin{aligned}
 F_1(\underline{k}, \underline{k}'), & \quad F_3(\underline{k}, \underline{k}') = F_1(\underline{k}, \underline{k}') e^{i(\underline{k} - \underline{k}') \left(\frac{a+b}{2} + 2d_z \right)} \\
 F_2(\underline{k}, \underline{k}') e^{i(\underline{k} - \underline{k}') d_z}, & \quad F_4(\underline{k}, \underline{k}') = F_2(\underline{k}, \underline{k}') e^{i(\underline{k} - \underline{k}') \left(\frac{a+b}{2} + 3d_z \right)},
 \end{aligned}$$

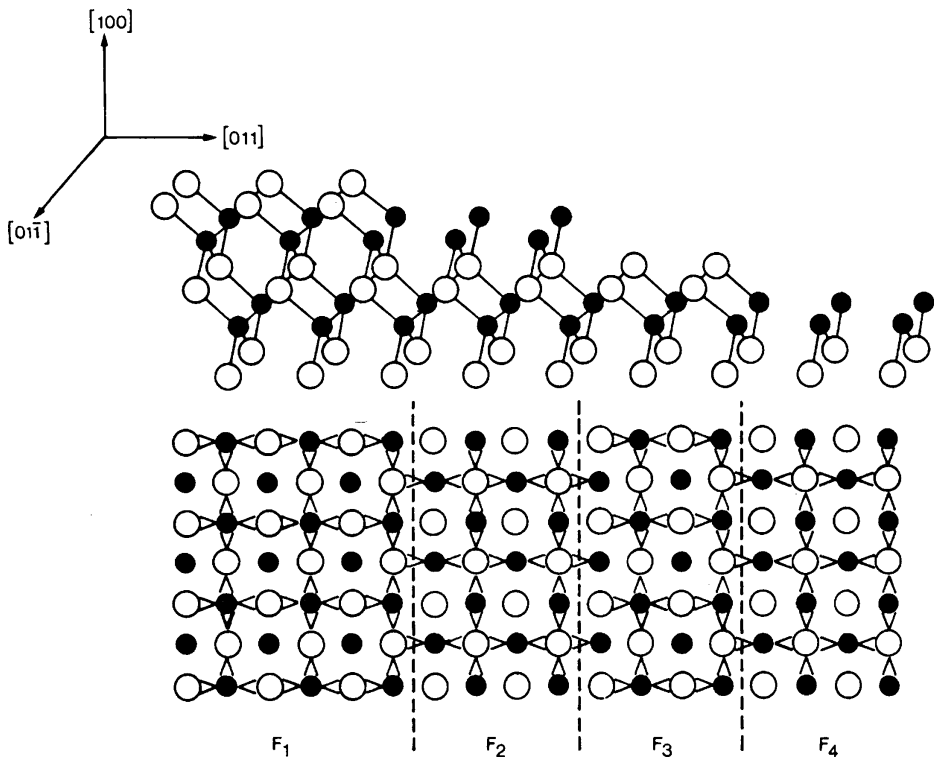


Fig. 5. Model of the Si(100) surface with four different terraces. The reconstruction of the surface is neglected here. The assignment of different structure amplitudes to the different atomic columns as used in the text is indicated in the Figure.

a and b are the lattice vectors of the primitive planar unit cell and d_z is the layer spacing. The reconstruction of the surface is neglected here because it is not relevant for the beam profiles of the specular beam. Multiple scattering events involving the edge atoms as well details of the atomic geometry near an edge are also not considered here. As mentioned above, at incidence in $[011]$ direction the structure factors F_1 and F_2 are different in modulus and phase even for the specular beam as the result of multiple scattering, while at incidence in $[010]$ this is not the case.

The phase factors due to the antiphase relation between terrace 1 and 3, and 2 and 4 respectively, as well as the phase factors due to the height differences are attributed here to the structure factors F_1 to F_4 . This is in general possible for a surface having only these four levels. For a rough surface with more levels this definition of the structure factors can be also used as long as only special diffraction conditions are considered. It is in general convenient to include the phase factors in the correlation matrix for the description of a rough surface [3]. However, the analytical evaluation of the eigenvalues for the general case becomes inconvenient here and the beam profiles may be calculated only for the special diffraction conditions of "in phase" and "out of phase" scattering from single and double steps.

There exists two different monoatomic steps at this surface. The atomic geometry at the edge from terrace 1 to terrace 2 differs from the step from terrace 2 to 3. Both steps are assumed here to occur with the same probability, for the sake of simplicity. To allow different

coverages for the terraces 1 and 2, and 3 and 4, respectively, the step down from terrace 1 to 2 may occur with probability α_1 and the step up from terrace 2 to 1 with probability α_2 . The assumption of different probabilities for these steps up and down enables the description of a surface with a preference for one kind of terraces. This is not unrealistic, because it has been experimentally observed that at vicinal faces one kind of terraces dominates [25-28]. The occurrence of double steps is given by the probability β . The edge of double steps is normal to the dimer rows in the (2×1) reconstructed surface, as it becomes visible in the splitting of superstructure spots at vicinal surfaces [25,26]. Therefore it may be assumed for simplicity that double steps occur only between the terraces 1 and 3. Double steps between terraces 2 and 4 would occur in the other direction and cannot be considered in the one-dimensional model. It is further assumed that double steps up and down occur with equal probability which ensures that the average orientation of the surface is in $[100]$. Because the probability for the occurrence of a single step has to be divided into two contributions, the probability for a single step downward from terrace 1 to 2, or upward from terrace 1 to 4, is $\alpha/2$. For double steps this distinction needs not to be made because the step from terrace 1 to 3 may be upward or downward. To use the same definition for the probabilities for single and double steps the double step gets the probability β and not $\beta/2$. More sophisticated models of the topography of the surface are possible, but then the evaluation of the correlation matrix has to be done numerically. It is further doubtful that a more detailed picture is useful within the limits of a model of a geometric distribution of terrace sizes.

The correlation matrix for the above described model is given by

$$P(1) = \begin{bmatrix} 1 - \alpha_1 - \beta & \frac{\alpha_1}{2} & \beta & \frac{\alpha_1}{2} \\ \frac{\alpha_2}{2} & 1 - \alpha_2 & \frac{\alpha_2}{2} & 0 \\ \beta & \frac{\alpha_1}{2} & 1 - \alpha_1 - \beta & \frac{\alpha_1}{2} \\ \frac{\alpha_2}{2} & 0 & \frac{\alpha_2}{2} & 1 - \alpha_2 \end{bmatrix} \quad (10)$$

With

$$\sum_i p_i P_{ik}(j) = p_k, \quad (11)$$

the total area of different terraces is obtained from the left eigenvector of the correlation matrix to the eigenvalue 1. The probabilities p being the coverages of the corresponding terraces, are

$$p_1 = p_3 = \frac{\alpha_2}{2(\alpha_1 + \alpha_2)}, \quad p_2 = p_4 = \frac{\alpha_1}{2(\alpha_1 + \alpha_2)}. \quad (12)$$

In this model the difference in the coverage between the two rotational domains depends solely on the relation between the probabilities α_1 and α_2 for the steps up and down. The double step probability only influences the size distribution for the different terraces.

In the 1-D case the pair-correlation for all distances are easily calculated by powers of the matrix $P(1)$. (See also a recent review article by H. Jagodzinski [30].) The beam profile as the Fourier transform of the pair correlations is given by

$$I(\underline{k}, \underline{k}') = G(k) \sum_j p_i p_{ik} (j) F_i F_k^* e^{-i(\underline{k} - \underline{k}')j\mathbf{a}}. \quad (13)$$

With

$$p_{ik} = P(1)_{ik}^j \quad (14)$$

and

$$p^j = U^{-1} \lambda^j U, \quad (15)$$

the diffracted intensity can be written in the form

$$I(\underline{k}, \underline{k}') = G(k) \sum_{i=1}^4 \sum_{k=1}^4 \sum_{r=1}^4 \sum_j^{-N, N} F_i F_k^* U_{ir}^{-1} U_{rk}^j \lambda_r^j e^{-i(\underline{k} - \underline{k}')j\mathbf{a}}. \quad (16)$$

Defining quantities $B_r(\underline{k}, \underline{k}')$ and $D_r(\underline{k}, \underline{k}')$

$$\sum_{i=1}^4 \sum_{k=1}^4 U_{ir}^{-1} U_{rk} F_i(\underline{k}, \underline{k}') F_k^*(\underline{k}, \underline{k}') = B_r(\underline{k}, \underline{k}') + iD_r(\underline{k}, \underline{k}') \quad (17)$$

the beam profile is finally given by

$$I(\underline{k}, \underline{k}') = \sum_r^{1,4} B_r(\underline{k}, \underline{k}') \frac{1 - |\lambda_r|^2}{1 - 2|\lambda_r| \cos((\underline{k} - \underline{k}')\mathbf{a} + \phi_r) + |\lambda_r|^2} - 2D_r(\underline{k}, \underline{k}') \frac{|\lambda_r| \sin((\underline{k} - \underline{k}')\mathbf{a} + \phi_r)}{1 - 2|\lambda_r| \cos((\underline{k} - \underline{k}')\mathbf{a} + \phi_r) + |\lambda_r|^2} \quad (18)$$

The eigenvalues of the matrix $P(1)$ are in general complex

$$\lambda_r = |\lambda_r| e^{i\phi_r}. \quad (19)$$

The phase ϕ_r of an eigenvalue describes the position of the maximum of the beam profile and the modulus $|\lambda_r|$ the width.

The first term in Eq. 18 describes a symmetric profile (in general the main contribution) and the second term describes an asymmetric correction. The origin of the asymmetric correction may be two-fold. For a symmetric distribution of up and down steps the kinematic beam profile is always symmetric and the quantities $D_r(\underline{k}, \underline{k}')$ vanish. This has been denoted also by the term "reversible" surface [7,8]. For a vicinal plane the probabilities of up and down steps are not equal in both directions ("irreversible surface") and the beam profiles become asymmetric. The second origin for an asymmetry of beam profiles is multiple scattering at the edges. Asymmetric profiles will not be discussed here.

The quantities $B_r(\underline{k}, \underline{k}')$ and $D_r(\underline{k}, \underline{k}')$ are linear combinations of the scattering amplitudes and may be also denoted as structure factors in the following. It is in general convenient to calculate the structure factors numerically by the eigenvectors of the matrix $P(1)$ according to Eq. 17. In simple cases, such as the two-level system discussed above, an analytic expression showing the relation to the coverage Θ is useful [4-8] but for the special case discussed here with four eigenvalues and four different

structure factors the expression of the structure factors in terms of the coverages becomes unhandy. However, the approximate analytic expression of the structure factors and the eigenvalues of the matrix $P(1)$ can be found for special diffraction conditions. Inspection of the eigenvalues λ_r and structure factors $B_r(\underline{k}, \underline{k}')$ at the "in phase" ($\cos(\underline{k} - \underline{k}')d = 1$) and "out of phase" ($\cos(\underline{k} - \underline{k}')d = -1$) diffraction condition for single steps shows the variation of beam intensities and profiles in reciprocal space. The four eigenvalues of the (4 x 4) matrix are:

$$\begin{aligned}\lambda_1 &= 1 \\ \lambda_2 &= 1 - \alpha_1 - \alpha_2 \\ \lambda_3 &= 1 - \alpha_1 - 2\beta \\ \lambda_4 &= 1 - \alpha_2\end{aligned}\tag{20}$$

The structure factors to the first two eigenvalues at in phase diffraction from all levels are

$$\begin{aligned}B_1(\underline{k}, \underline{k}') &= \left| \sum_i p_i F_i(\underline{k}, \underline{k}') \right|^2 \\ B_2(\underline{k}, \underline{k}') &\sim p_1 p_2 \left| F_1(\underline{k}, \underline{k}') - F_2(\underline{k}, \underline{k}') \right|^2.\end{aligned}$$

The other two structure factors turn out to be very small, because $|F_1| = |F_3|$ and $|F_2| = |F_4|$. Therefore the contributions from λ_3 and λ_4 become very weak and the beam profile consists of two parts, a central spike and a broad profile. The intensity of the central spike is proportional to the average structure factor and the diffuse part is due to the mean square deviations, as discussed above. At the out of phase condition for single steps the beam profile consists also of two parts with the reverse relation between the intensities. At the out of phase condition for double steps, $\cos(\underline{k} - \underline{k}')d = 0$, the central spike and the broad profile for λ_2 vanish and the two broadened profiles from the two eigenvalues λ_3 and λ_4 become intensive. The relative intensities can be calculated from Eq. 17, the analytic expression being not very instructive is not given here

The qualitative picture for incidence along [011] is given in Figure 6. The beam profiles show a double periodicity in reciprocal space corresponding to the double step height. At the "in phase" condition for a single step all terraces scatter in phase and the width of the diffuse intensity shows the single terrace width. The diffuse intensity arises from the different scattering factors of the two rotational domains. The same occurs for the "out of phase" condition for a single step. The terraces 1 and 3, or 2 and 4 respectively, are then in phase and the diffuse intensity again shows the average terrace width. In between the diffuse intensity consists of a superposition of two Lorentzian profiles, the narrower one showing the average width of the two terraces, and the other one showing an additional broadening from which the probability β for double steps can be obtained.

The beam profiles for a surface having only single steps is shown for comparison in Figure 7. Assuming only the one probability α for a single step, all terraces occur with equal probability. The width of the diffuse intensity shows also a double periodicity in reciprocal space, that is because there are four different terraces at the surface. The double periodicity of the beam widths has been experimentally observed at a surface where single steps were obviously predominant [17]. The central spike does not vanish at the "out of phase" condition for single steps because of the different structure factors for the two rotational domains. At (001), (003) etc. ($s = 1/4, 3/4$ etc.) the diffuse intensity becomes narrower because then the average repeat distance is twice the average terrace size. The central spike vanishes at all diffraction conditions

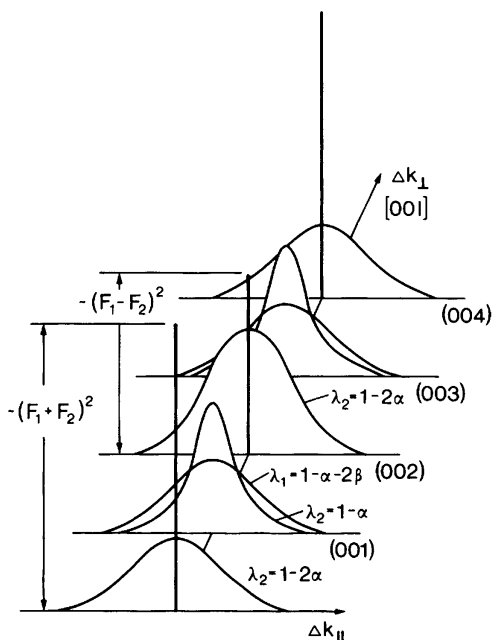


Fig. 6. Schematic drawing of the variation of the angular profiles of the specular beam for a Si(100) surface exhibiting single and double steps. A geometrical distribution of terrace sizes has been assumed with equal probability α for single steps up or down, and β for double steps. The "in phase" condition for double steps is at (002), (004), while (002) is the "out of phase" condition for single steps. The eigenvalue λ of the correlation matrix indicated in the Figure determines the widths of the diffuse intensities. The incident beam has been assumed along the [011] direction.

except at the "in phase" and "out of phase" condition for single steps because a multi-level system has been assumed by allowing up and down steps at all levels.

CONCLUSIONS

It has been shown that at surfaces with non-equivalent terraces the intensity oscillations in reciprocal space and as a function of coverage may differ substantially from the simple case where only antiphase domains exist. For a quantitative evaluation of beam profiles multiple scattering effects cannot be neglected and also the orientation of the incident beam has to be considered. For a Si(100) surface with four different terraces and a certain model for double steps the beam profiles have been theoretically described. The beam profile exhibits at the "in phase" and "out of phase" condition for single steps a diffuse intensity with a width according to the single step probability. If double steps are present at the surface with a considerable probability the corresponding broadening of the beam becomes visible at a momentum transfer normal to the surface of $s = 1/4, 3/4$ in reciprocal units, which the "out of phase" condition for double steps. The profile consists then of a superposition of two Lorentzian profiles with different widths. The probabilities for double

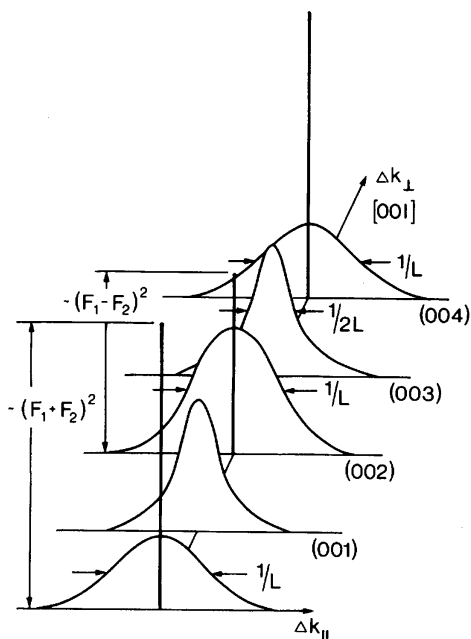


Fig. 7. Same as Figure 6 for a surface having only single steps.

steps can be determined if both components can be separated. The existence of two diffuse components should be indicated by deviations from the Lorentzian shape of the profile. This should be also observable at incidence in [010] direction where the structure factors for the two rotational domains become equal. The beam profile would then also deviate from the Lorentzian shape.

Acknowledgement

The author would like to thank Prof. M. G. Lagally, Dr. D. Saloner, J. Martin and D. Savage for stimulating discussions. Part of this work was completed at the Dept. of Metallurgical Engineering, Univ. Wisconsin-Madison with support from ONR, Chemistry Program. Financial support of the Deutsche Forschungsgemeinschaft (SFB 128) is also gratefully acknowledged.

REFERENCES

1. M. Henzler, Surface Sci., 22:12 (1979).
2. M. Henzler, Electron diffraction and surface defect structure, in: "Electron Spectroscopy for Surface Analysis", H. Ibach, ed., Springer Verlag, Berlin-Heidelberg-New York (1977).
3. H. Jagodzinski, W. Moritz and D. Wolf, Surface Sci., 77:233 (1978).
W. Moritz, H. Jagodzinski and D. Wolf, Surface Sci., 77:249 (1979).
D. Wolf, H. Jagodzinski and W. Moritz, Surface Sci., 77:265 (1979).
D. Wolf, H. Jagodzinski and W. Moritz, Surface Sci., 77:283 (1979).
4. T. M. Lu and M. G. Lagally, Surface Sci., 120:47 (1982).
5. T. M. Lu, G.-C. Wang and M. G. Lagally, Surface Sci., 108:494 (1981).
6. J. M. Pimbley and T. M. Lu, J. Appl. Phys., 55:182 (1984).
J. M. Pimbley and T. M. Lu, J. Appl. Phys., 57:1121 (1985).
J. M. Pimbley and T. M. Lu, J. Appl. Phys., 58:2184 (1985).

7. C. S. Lent and P. I. Cohen, Surface Sci., 139:121 (1984).
8. P. R. Pukite, C. S. Lent and P. I. Cohen, Surface Sci., 161:39 (1985).
9. M. G. Lagally, D. E. Savage and M. C. Tringides, this volume, p. 139.
10. J. Zhang, J. H. Neave, P. J. Dobson and B. A. Joyce, Appl. Phys., A42:317-326 (1987).
11. T. Sakamoto, N. J. Kawai, N. J. Kagakawa, K. Ohta and T. Kojima, Appl. Phys. Lett., 47:617-619 (1985).
T. Sakamoto, T. Kawamura and G. Hashiguchi, Appl. Phys. Lett., 48 (1986).
12. J. Aarts, W. M. Gerits and P. K. Larsen, Appl. Phys. Lett., 48:931 (1986).
13. B. A. Joyce, J. H. Neave, J. Zhang and P. J. Dobson, this volume, p. 397.
14. J. M. Cowley, "Diffraction Physics", Elsevier Science Publ., Amsterdam-New York (1981).
15. W. Moritz, Inst. Phys. Conf. Ser., 41:261 (1978).
16. M. Henzler, this volume, p. 193.
17. J. A. Martin, C. E. Aumann, D. E. Savage, M. C. Tringides, M. G. Lagally, W. Moritz and F. Kretschmar, J. Vac. Sci. Technol. (1986).
18. M. Horn, U. Gotter and M. Henzler, this volume, p. 463.
19. T. Kawamura, T. Sakamoto and K. Ohto, Surface Sci., 171:L409-L414 (1986).
20. D. Saloner, J. A. Martin, M. C. Tringides, D. E. Savage, C. A. Aumann and M. G. Lagally, J. Appl. Phys., 61:2884 (1987).
21. H. Saalfeld, S. Tougaard, K. Bolwin and M. Neumann, Surface Sci. (1986).
22. T. Sakamoto, N. J. Nagakawa, K. Ohta and T. Kojima, Appl. Phys. Lett., 47:617-619 (1985).
23. S. B. Hendricks and E. Teller, J. Chem. Phys., 10:147 (1942).
24. H. Jagodzinski, Acta Cryst., 2:201, 208 and 298 (1949).
25. J. Kakinoki and Y. Kamura, J. Phys. Soc. Japan, 9:169, 176 (1954).
26. M. Henzler and J. Clabes, Proc. 2nd Intern. Conf. on Solid Surfaces 1974, Japan. J. Appl. Phys., Suppl. 2, Pt. 2:389-396 (1974).
27. R. Kaplan, Surface Sci., 93:145-158 (1980).
28. N. Inoue, Y. Tanishiro and K. Yagi, Japan. J. Appl. Phys., 26:L293 (1987).
29. T. Nakayama, Y. Tanishiro and K. Takanayagi, Japan. J. Appl. Phys., 26:L280 (1987).
30. D. E. Aspnes and J. Ihm, Phys. Rev. Lett., 57:3054-3057 (1986).
31. H. Jagodzinski, Prog. Crystal Growth and Charact., 14:47-102 (1987).

INDEX

- Adatom migration during growth, 409
- Aluminium arsenide
 - growth by MBE using phase lock modulated beams, 419
- Antimony
 - grown on GaAs(110), 482
- Atomic steps
 - effect on rocking curves, 511, 516
 - kinematic diffraction, 428
 - RHEED, 427, 504
- Auger electron emission, 109, 117
- Beam - Specimen interaction, 325
- Channelling effects, 117
 - in Reflection Electron Microscopy, 274
- Column approximation and REM, 268
- Convergent Beam Diffraction
 - surface characterisation, 237
 - surface multislice approach, 251
- Copper oxidation, 320
- Defects and Disorder, 139, 201, 217
 - multilevel systems, 157
 - steps, 175, 193, 217
 - surface roughness and 3-D structure, 160
 - two level systems, 146
 - vicinal surfaces, 154
- Depth of focus in REM, 269
- Diffuse scattering, 177
 - thermal diffuse scattering, 211
- Dislocations
 - contrast in REM, 329, 332
 - resonance condition, 338
- Disorder, 33
 - in Si(100)(2xn), 533
- Dynamical Theory in RHEED, 29, 43, 31
 - resonances, 100
- Electron Microscopy of Surfaces
 - with Low Energy Electrons, 381, 385
 - reflection, 77, 261, 285, 303, 317, 329, 343
- Gallium Arsenide
 - growth by MBE, 397
 - growth using phase-lock modulated beams, 419
 - growth of Antimony on, 482
 - (001) surface, 49, 204, 318, 508
 - (110) surface, 72, 276, 390, 530
 - reflection microscopy, 84, 318
 - thermal annealing, 530
- Germanium
 - (001) surface, 217
 - RHEED from growing surface, 449
- Gold surfaces studied by REM, 303, 315
- Growth kinetics, 163, 523
 - annealed GaAs(110), 530
 - disorder of Si(100)(2xn), 533
 - oxygen p(2x1) overlayers on W(110), 527
- Growth of metals on GaAs(110), 475
- Growth modes, 362, 493
- Growth Processes, 407, 456, 476
 - effect of interruption, 414
- Image formation in REM, 268, 285, 296
- Indium on GaAs(110), 482
- Inelastic scattering in RHEED
 - phonons, 38
 - plasmons, 39
 - resonance conditions, 277
- Interrupted Growth, 414
- Ion bombardment damage, 217
- Kikuchi effects, 201, 403, 437
- Low Energy Electron Diffraction,
 - intensity oscillations, 466
 - Si MBE on Si(001), 463
 - spot profile, 467
- Low Energy Electron Reflection Microscope, 381
- Low Energy Electron Scanning Microscope, 385

Metal Epitaxy, Overlayers etc..
 phase transformations, 11
 superstructures, 11
 Ag/Si, 15, 17
 Al/Si, 351
 Au/Si, 9, 11, 16, 18, 349
 Cu/Nb, 489
 Cu/Ni, 489
 Cu/W, 489
 In/Ge, 16, 17
 In/GaAs, 482
 Mo/W, 489
 Nb/W, 489
 Ni/Si, 17
 Ni/Mo, 489
 Ni/W, 489
 Sb/GaAs, 482
 Sn/Ge, 19, 17
 Microprobe RHEED, 343
 Molecular Beam Epitaxy
 AlGaAs, 412, 443
 GaAs, 201, 397, 419, 435
 Ge, 443, 449
 metals, 489
 Si, 355, 449, 463
 surface structures during growth,
 367
 Monolayer scattering, 101, 103
 Multilevel systems, 157

 Nickel deposited onto silicon, 373

 Oxidation studies of copper, 320

 Penetration depth, 80, 81
 Phase-lock modulated beams in MBE,
 419
 Photoemission
 angle resolved, of surface during
 growth, 452
 Platinum
 (111) surface, 104, 109, 213, 281
 gold deposited on Pt(111), 285
 reflection electron microscopy,
 281, 303, 312, 330

 Reconstructed surfaces studied with
 RHEED, 3, 43
 Reflection Electron Microscopy, 77,
 261, 285, 303, 317, 329, 343
 column approximation, 268
 contrast of steps, 329
 facetting, 307
 image computations, 86
 image formation, 267
 inelastic scattering, 277, 287
 resonance effects, 274
 specimen preparation, 279
 in STEM, 261, 317
 in TEM, 261
 surface defects, 85
 Reflection High Energy Electron
 Diffraction (RHEED)
 apparatus, 4
 atomic steps, effect of, 427
 Bloch wave formulation, 131, 270
 disorder, 32, 33, 139, 201
 dynamical theory, 29, 34, 43, 63,
 131
 elastic scattering, 30
 inelastic scattering, 38, 109
 intensity oscillations, 165, 208,
 356, 397
 apparent phase shift, 401, 492
 damping, 495
 diffraction conditions 399, 453,
 510
 dynamical theory, 492
 low growth temperature, 450
 metal epitaxy, 489
 phase-lock modulated beams, 419
 residual gas effects, 496
 theoretical modelling, 501
 integral formulation, 131
 invariant imbedding method, 67
 kinematic theory, TDS, 212
 microprobe, 343
 multiple scattering, 506
 multi-slice method, 271
 novel techniques, 6
 oscillation/rotation patterns, 8
 patterns, interpretation, 4
 reconstructed surfaces, 3, 43
 resonance effects, 99
 rocking curves, 52, 63, 104
 streaks, 241
 streak shape, 208
 surface structure determination,
 29
 symmetry, 242
 thermal diffuse scattering, 211
 three level system, 517
 two level system, 429
 vicinal surfaces, 432
 x-ray spectroscopy, 20
 Resonance conditions in RHEED, 83,
 99
 contrast of steps in REM, 329, 331
 contrast of dislocations in REM,
 339
 defect images, 279
 dynamical theory, 100, 109, 122
 reflection electron microscopy, 274
 Rough surfaces by REM, 319

Scanning microprobe for REM, 385
 Scanning transmission electron microscope for REM, 317
 Scanning tunnelling microscope, 391
 Secondary electron emission, 109, 118
 Silicide formation observed by UHV SEM, 371
 Silicon,
 growth studies by RHEED, 449, 513
 by low energy electron microscopy, 381, 388
 by reflection electron microscopy, 303
 substrate cleaning, 354
 Si(001), 185
 growth, 463, 513
 (2xn) phase, 533
 Si(110), 389
 Si(111), 5, 12, 195, 347, 352, 374
 Si(111) + Au (5x1), 9, 11
 Silver,
 (001) RHEED calculation, 71
 surfaces by REM, 303, 315
 Specimen preparation for REM, 279, 292, 303, 334
 Steps,
 contrast in REM, 329, 335
 electron diffraction, 193
 electron scattering, 175
 Superlattices,
 RHEED oscillations during growth of, 496
 Surface defects, 85
 Surface phase transformations, 11, 225
 Surface reconstruction, 3
 REM of the (111)Au surface, 297
 Surface roughness, 160
 Surface structure determination, 3, 29, 43
 Surface superstructures
 metal induced on Si and Ge, 13, 18
 Surface wave resonance, 99, 109, 122
 Time dependent changes of RHEED, 163, 208 (see also RHEED Intensity Oscillations)
 Total Reflection Angle X-ray Spectroscopy (TRAXS), 22
 Two Level Systems, 146
 Ultra high vacuum electron microscope, 289, 371
 Vicinal Surfaces, 154
 diffraction from, 432
 GaAs and Ge, 440
 X-ray spectroscopy and RHEED, 20

